

## Supporting Information

# Extending Shell-Isolated Nanoparticle-Enhanced Raman Spectroscopy Approach to Interfacial Ionic Liquids at Single Crystal Electrode Surfaces

Meng Zhang, Li-Juan Yu, Yi-Fan Huang, Jia-Wei Yan, Guo-Kun Liu, De-Yin Wu,\*Zhong-QunTian, Bing-Wei Mao\*

E-mails: bwmao@xmu.edu.cn, dywu@xmu.edu.cn

### 1. Experimental details

BMIPF<sub>6</sub> and OMIPF<sub>6</sub> were purchased from IoLiTec (Germany) at purity of 99%. Prior to each measurement, ionic liquids were dried in vacuum at 80 °C for several hours in the glove box filled with ultra pure N<sub>2</sub> (99.999%) to remove adsorbed water and oxygen. Pinhole-free Au@SiO<sub>2</sub> nanoparticles with Au core diameter of ~55 nm and SiO<sub>2</sub> shell thickness of ~3 nm (as shown in Figure S1) were prepared according to the work by Li et al<sup>1</sup>.

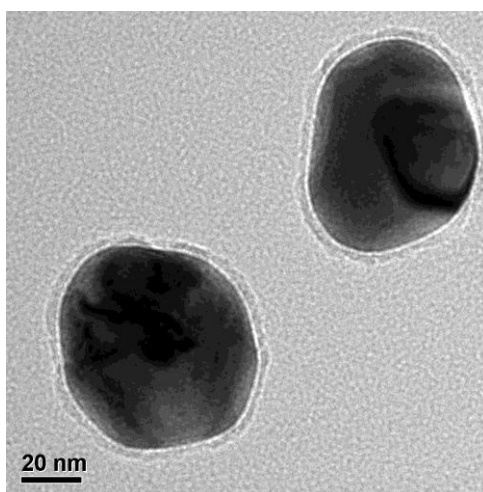


**Figure S1.** HRTEM image of Au@SiO<sub>2</sub> NPs.

Raman experiments were carried out on a confocal microscopy Raman instrument (Invia, Renishaw, UK) using excitation line of 632.8 nm from He-Ne laser. Electrochemical control was fulfilled using a CHI electrochemical workstation (CHI814, CH Instrument). The (111) facets of

Au single crystal beads were prepared following Clavilier's method<sup>2</sup> and used as working electrodes for Raman measurements. Au@SiO<sub>2</sub> NPs were introduced by dropping a dilute Au@SiO<sub>2</sub> sol solution onto the Au single crystal facets, followed by evaporation of the solvent water in the sol. Two platinum wires were used as the counter and quasi-reference electrodes, respectively. After each experiment, the potential of the Pt quasi-reference electrode was calibrated against a saturated calomel electrode (SCE). All of the potentials reported in this work were versus the Pt quasi-reference which was ~0.3 V against the SCE.

## 2. DFT calculation details

Density functional calculations were carried out with Becke's three-parameters hybrid exchange functional and Lee-Yang-Parr correlation functional approach B3LYP.<sup>3</sup> The basis sets for C, N, and H atoms of investigated molecules were 6-311+G(d, p), which included the polarization function in all the atoms and diffuse function in C, and N atoms.<sup>4</sup> The theoretical method used has been proven suitable in investigating vibrational frequency, and Raman activity of pyridine interacting with water clusters and coinage metal clusters.<sup>5,6</sup> All the above quantum chemical calculations, including geometry optimizations, analytic frequencies, Raman scattering factors, and polarizability derivative were carried out by using Gaussian 09 package.<sup>7</sup>

The scaled quantum mechanics force field (SQMF) procedure<sup>8</sup> was used to analyze vibrational bands of all fundamentals. The calculated frequencies were scaled by the factor of 0.981 for below 2000 cm<sup>-1</sup> and 0.963 for above 2000 cm<sup>-1</sup>. The vibrational bands are assigned according to the potential energy distribution (PED) using the equilibrium geometries and the Cartesian force constant matrix calculated at the B3LYP/6-311+G (d, p) level. Differential Raman scattering cross sections (DRSC) are calculated on top of Raman scattering factors (RSF), as published in our previous work.<sup>9</sup> In order to make direct comparison with the normal Raman spectra (NRS), the calculated Raman spectra were presented in terms of the Lorentzian expansion of the DRSC magnitudes.

Raman scattering factors contains two contributions, the isotropic polarizability derivative and the anisotropic polarizability derivative of the vibrational mode. This means Raman intensity is

proportional to the square of polarizability derivative.  $a_{JK}(J, K = X, Y, Z)$  is the element of the second rank polarizability tensor  $\hat{a}$ .  $\hat{a}$  is a symmetrical tensor ( $a_{JK} = a_{KJ}$ ) and, therefore, has six independent components only ( $a_{XX}, a_{XY}, a_{XZ}, a_{YY}, a_{YZ}$  and  $a_{ZZ}$ ). The components depend on the space orientation of the molecule but not on the electric applied. In order to get the influence of photoelectric field on the Raman intensities of certain vibrational modes of the molecule, as known as the changing of the orientation of molecule on the surface of gold, we need to convert the molecule-fixed coordinates (x, y, and z) to space-fixed coordinate system (X, Y, and Z). Since all molecules contribute to the intensity of the scattered radiation, it is necessary to average the components of  $\hat{a}$  over all possible orientations of the molecule-fixed axes x, y, and z with respect to the inertial (laboratory) Cartesian frame X, Y, and Z. We assume that the photoelectric field (i.e. Z axes of the space-fixed coordinate system) is perpendicular to the surface of gold. Thus,  $a_{ZZ}$ , the polarizability tensor at zz direction that is normal to the surface, can be used to compare the Raman intensity of the adsorbed molecule with different orientations.

### 3. Vibrational assignments of the main bands of BMI<sup>+</sup>.

**Table S1.** B3LYP (6-311+g\*\*) Vibrational assignments of the main bands of BMI<sup>+</sup>

$\nu_{\text{calc.}}(\text{cm}^{-1})$	$\nu_{\text{exp.}}(\text{cm}^{-1})$	Description(%)
1020	1025	Str N <sub>3</sub> C <sub>4</sub> (30),R5 def'(33)
1035	1055	Str C <sub>7</sub> C <sub>8</sub> (19),C <sub>8</sub> C <sub>9</sub> (37),C <sub>9</sub> C <sub>10</sub> (34)
1108	1117	Str C <sub>8</sub> C <sub>9</sub> (15),Rock C <sub>10</sub> H (33)
1311	1306	Twl C <sub>8</sub> H(43),C <sub>9</sub> H(48)
1330	1340	Str N <sub>3</sub> C <sub>4</sub> (16),N <sub>3</sub> C <sub>6</sub> (16),N <sub>1</sub> C <sub>7</sub> (11),Twl C <sub>7</sub> H(10)
1386	1390	Str N <sub>3</sub> C <sub>4</sub> (12),N <sub>3</sub> C <sub>2</sub> (25),Sym def C <sub>6</sub> H(11),Rock C <sub>7</sub> H(10)
1415	1420	Str C <sub>4</sub> C <sub>5</sub> (11),N <sub>1</sub> C <sub>5</sub> (18),N <sub>1</sub> C <sub>2</sub> (22),Twl C <sub>7</sub> H(21)
1461	1450	Sci C <sub>7</sub> H(24),C <sub>8</sub> H(57),C <sub>9</sub> H(14)
1576	1568	Str C <sub>4</sub> C <sub>5</sub> (34),N <sub>3</sub> C <sub>2</sub> (25),bend C <sub>4</sub> H(14)
2917	2880	Str C <sub>8</sub> H(24),C <sub>9</sub> H(75)
2934	2919	Str C <sub>10</sub> H(92)
2940	2944	Str C <sub>8</sub> H(25), C <sub>9</sub> H(70)
2974	2974	Str C <sub>6</sub> H(100)
3185	3184	Str C <sub>4</sub> H(43),C <sub>5</sub> H(52)

Note: str = stretching, bend = bending, rock = rocking, twi = twisting, sci = scissoring, R5 def' = 5-ring deformation', symdef = symmetry deformation. The number in parentheses indicates the percentage of the vibration mode (Vibration modes with less than ten percent proportion are ignored).

#### 4. CV results of Au(111) in BMIPF<sub>6</sub> and OMIPF<sub>6</sub>

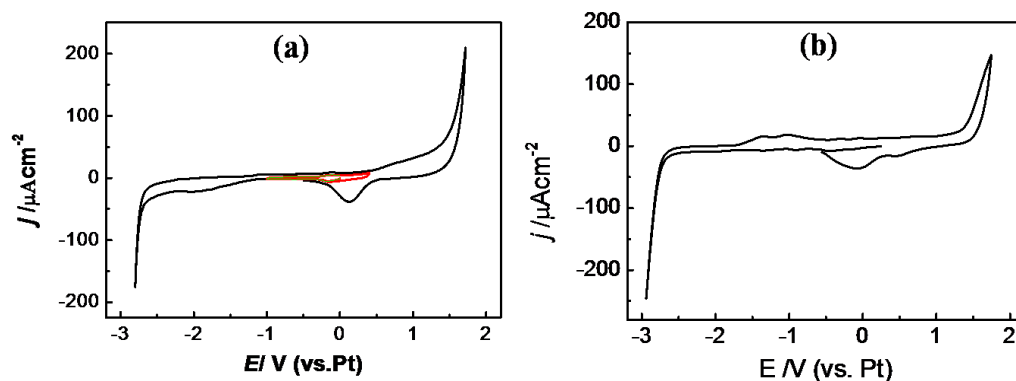


**Figure S2.** CVs of Au(111) in (a) BMIPF<sub>6</sub> and (b) OMIPF<sub>6</sub> at scan rate of 50 mV/s.

#### 5. SHINERS results of BMIPF<sub>6</sub> on Au(100)

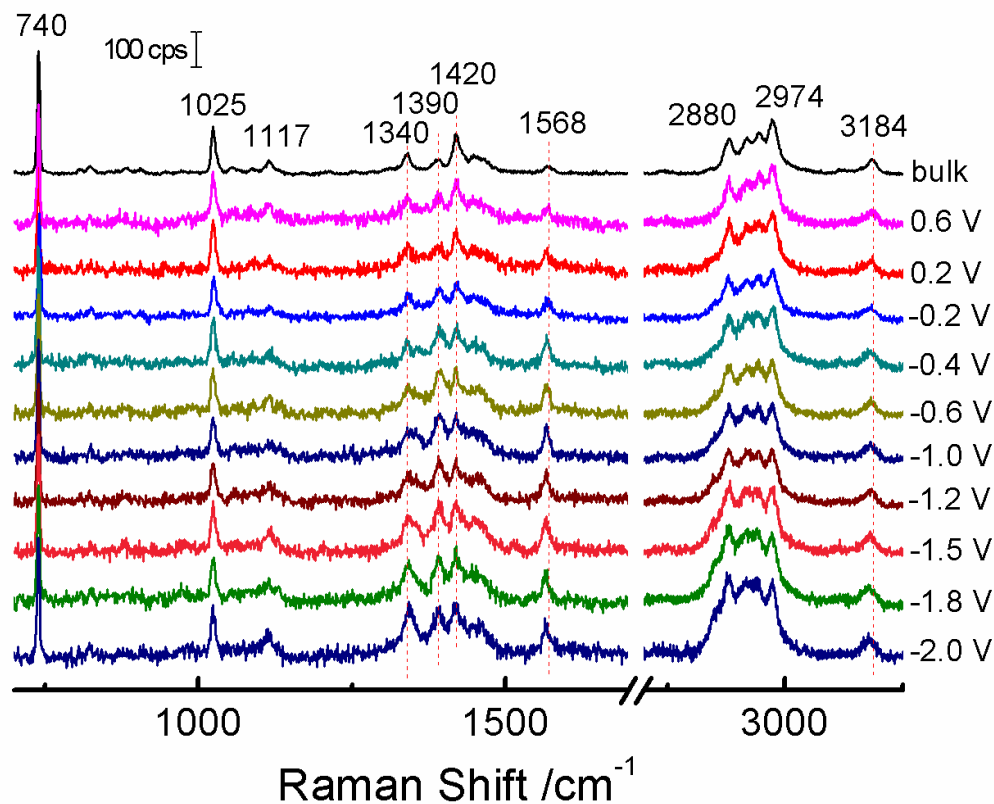


**Figure S3.** Potential-dependent Raman spectra of BMIPF<sub>6</sub> on Au(100) with Au@SiO<sub>2</sub> NPs. Laser power: 0.4 mW; collecting time: 10s. (PZC = -0.25 V, vs. Pt wire.<sup>10,11</sup>)

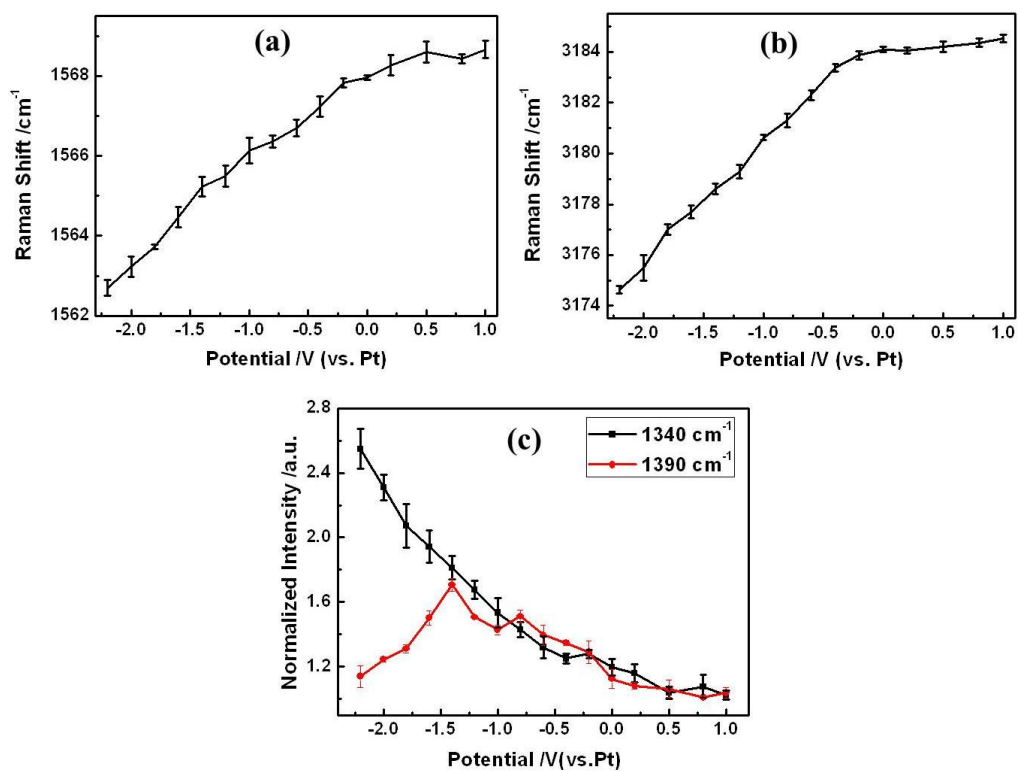


**Figure S4.** Potential-dependent Raman shift of 1568 cm<sup>-1</sup> (a) and 3184 cm<sup>-1</sup> (b) bands and potential-dependent normalized intensity of 1340 and 1390 cm<sup>-1</sup> bands (c) of BMIPF<sub>6</sub> on Au(100).

## 5. SHINERS results of OMIPF<sub>6</sub> on Au(111)

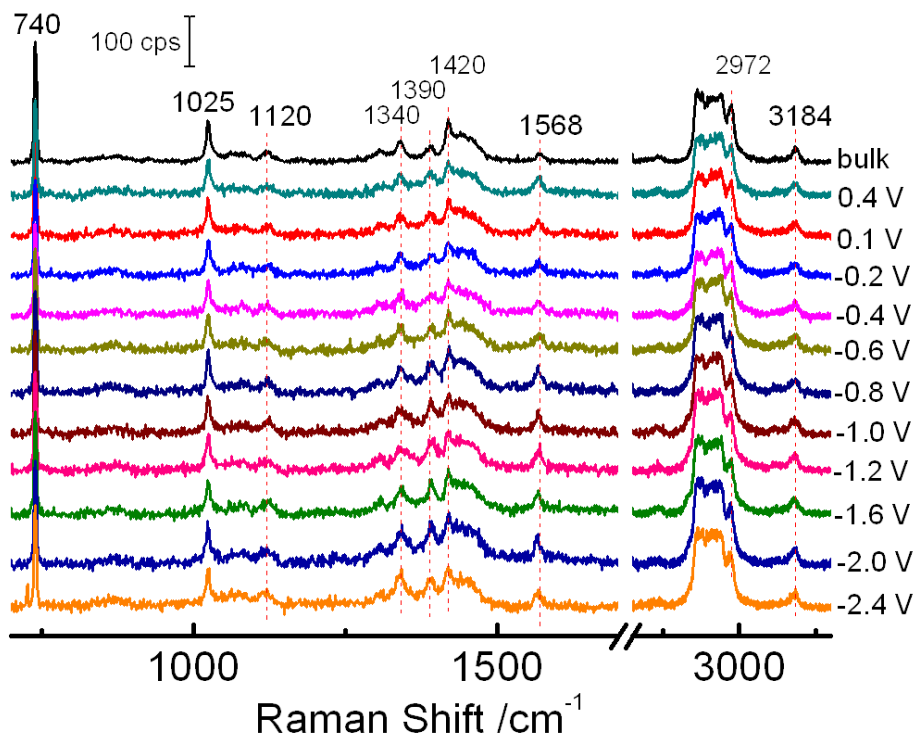


**Figure S5.** Potential-dependent Raman spectra of OMIBF<sub>6</sub> on Au(111) with Au@SiO<sub>2</sub> NPs. Laser power: 0.4 mW; collecting time: 20s. (PZC = -0.7V, vs. Pt wire.<sup>12</sup>)

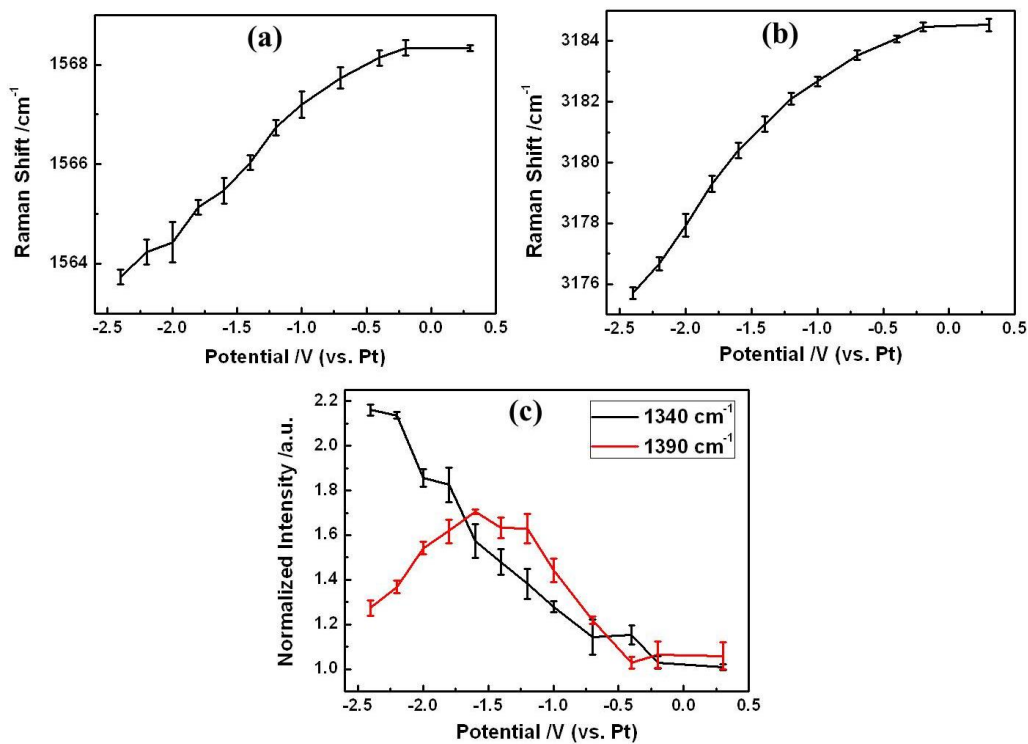


**Figure S6.** Potential-dependent Raman shift of 1568 cm<sup>-1</sup> (a) and 3184 cm<sup>-1</sup>(b) bands and

potential-dependent normalized intensity of 1340 and 1390  $\text{cm}^{-1}$  bands (c) of OMIPF<sub>6</sub> on Au(111).

## References

- 1 J. F. Li, Y. F. Huang, Y. Ding, Z. L. Yang, S. B. Li, X. S. Zhou, F. R. Fan, W. Zhang, Z. Y. Zhou, Y. W. De, B. Ren, Z. L. Wang and Z. Q. Tian, *Nature*, 2010, **464**, 392.
- 2 J. Clavilier, R. Faure, G. Guinet and R. Durand, *J. Electroanal. Chem.*, 1980, **107**, 205.
- 3 A. D. Becke, *J. Chem. Phys.* 1996, **104**, 1040.
- 4 M. Muniz-Miranda, B. Pergolese and A. Bigotto, *J. Phys. Chem. C*, 2008, **112**, 6988.
- 5 D. Y. Wu, X. M. Liu, S. Duan, X. Xu, B. Ren, S. H. Lin and Z. Q. Tian, *J. Phys. Chem. C*, 2008, **112**, 4195.
- 6 L. J. Yu, R. Pang, S. Tao, H. T. Yang, D. Y. Wu and Z. Q. Tian, *J. Phys. Chem. A*, 2013, **117**, 4286.
- 7 M. Frisch, G. Trucks, H. Schlegel, G. Scuseria, M. Robb, J. Cheeseman, G. Scalmani, V. Barone, B. Mennucci and G. Petersson, Gaussian 09 Revision A. 02, 2009, Gaussian Inc. Wallingford CT 2009.
- 8 A. K. Chandra, M. T. Nguyen, T. Uchimaru and T. Zeegers-Huyskens, *J. Phys. Chem. A*, 1999, **103**, 8853.
- 9 D. Y. Wu, M. Hayashi, S. H. Lin and Z. Q. Tian, *Spectrochim. Acta Mol. Biomol. Spectros.*, 2004, **60**, 137.
- 10 M. Gnahm, C. Muller, R. Repanszki, T. Pajkossy and D. M. Kolb, *Phys. Chem. Chem. Phys.*, 2011, **13**, 11627.
- 11 M. Gnahm, T. Pajkossy and D. M. Kolb, *Electrochim. Acta*, 2010, **55**, 6212.
- 12 Y. X. Zhong, J. W. Yan, M. G. Li, X. Zhang and B. W. Mao, unpublished result.